ORIGINAL ARTICLE

Selective fabrication of hollow and solid polysaccharide composite fibers using a microfluidic device by controlling polyion complex formation

Kazutoshi Iijima[1,2,3] · Shun Ohyama[2] · Kazuya Yuyama[2] · Atsushi Shono[1,2] · Mineo Hashizume[1,2]

Abstract

Natural polysaccharides are an important class of biomaterials that have attracted significant research interest for biomedical applications because of their high biocompatibility, biodegradability, and bioactivity. In this work, we fabricated water-insoluble composite hollow and solid fibers made of polyion complexes of chondroitin sulfate C (CS) and chitosan (CHI) using a single microfluidic device. A coaxial two-phase microfluidic device was constructed from stainless-steel needles and glass fibers, and CHI solutions and CS solutions were continuously infused into the core and sheath channels, respectively. The obtained fibers were flexible and homogeneous and had diameters of a few hundred micrometers. Hollow fibers were formed using water as the solvent of CS, while core-filled solid fibers were obtained using 20% (v/v) ethanol. The respective mechanisms for the fabrication of the hollow and solid fibers were discussed. An increase in the sheath flow rate or decrease in the core flow rate reduced the diameters of the fibers, while a reduction in the concentration of the CHI solution reduced the thickness of the hollow fibers. Furthermore, bovine serum albumin, used as a model protein, could be incorporated in the hollow and solid fibers by mixing them in the core flow solution. These results suggested the great potential of microfluidic techniques for the preparation of hollow and solid polysaccharide fibers.

Introduction

Fibers, which are two-dimensional bendable materials, have been widely used in the biomedical field. Core-filled solid fibers have been used as not only absorbable surgical sutures but also as component units of cell scaffolds for the construction of more complex objects, such as textile fabrics and three-dimensional structures. For example, three-dimensional scaffolds for cartilage tissue regeneration were fabricated from fibers of bioabsorbable polymers [1], and functional woven tissues were assembled from cell-laden biopolymer fibers [2]. On the other hand, hollow fibers have

been used for regeneration of the peripheral nerve gap [3], construction of artificial blood vessels [4], and bioreactors for large-scale cell culture [5].

Natural polysaccharides are an important class of biomaterials that have attracted significant research interest because of their high biocompatibility, biodegradability, and bioactivity [6]. Fibers have been fabricated from single or multiple polysaccharides. Fibers made of single polysaccharides, such as chitin [7] and chitosan (CHI) [8, 9], have been prepared by wet spinning. Fibers and nonwoven fabrics of chitin and CHI have also been prepared by electrospinning [10, 11]. For the fabrication of composite fibers made of multiple polysaccharides, the use of polyion complexes (PICs) of anionic and cationic polysaccharides is a promising approach because it makes water-soluble polysaccharides water-insoluble without the use of cross-linking agents or chemical modification. Composite fibers made of

✉ Mineo Hashizume
mhashizu@ci.kagu.tus.ac.jp

1 Department of Industrial Chemistry, Faculty of Engineering, Tokyo University of Science, 12-1 Ichigayafunagawara-machi, Shinjuku-ku, Tokyo 162-0826, Japan

2 Graduate School of Chemical Sciences and Technology, Tokyo University of Science, 12-1 Ichigayafunagawara-machi, Shinjuku-ku, Tokyo 162-0826, Japan

3 Present address: Faculty of Engineering, Yokohama National University, 79-5 Tokiwadai, Hodogaya-ku, Yokohama 240-8501, Japan

PICs of polysaccharides can be prepared by the interface spinning method [12–14] and the spray spinning method [15] from anionic polysaccharides, such as gellan gum [12], gellan sulfate [13], chondroitin sulfate C (CS) [14], alginic acid (ALG) [15], and cationic CHI. In the interface spinning method, fibers are spun by withdrawing the films made of their PICs formed at the interfaces between the solutions of anionic and cationic polysaccharides. Although fibers can be obtained without an expensive apparatus, it is difficult to achieve continuous spinning and control the fiber diameter. In addition, hollow fibers cannot be obtained using conventional interfacial spinning methods.

Over the last decade, microfluidic techniques have gained popularity in the biomedical field [16] and have been applied for the continuous fabrication of fibers made of biomacromolecules [17–22]. In microfluidic spinning, coaxial flows stabilize laminar flows and solidification starts at the interfaces between the core flow and the sheath flow when the respective flows contain molecules and/or ions that react with each other, in some cases with the help of other stimuli, to form insoluble products. Continuous solidification by flowing resulted in the formation of fibers. If solidification occurs only at the very close regions of the interface between the core and sheath flows, hollow fibers are produced. On the other hand, when solidification proceeds into the center of the coaxial flow, core-filled fibers are obtained. Solidification processes have been mainly based on cross-linking, such as enzymatic cross-linking [18], photopolymerization [19] and the formation of electrolyte complexes, such as ALG and Ca^{2+} [20–22] and sodium triphosphate pentabasic and CHI [23]. However, to the best of our knowledge, the fabrication of fibers based on the formation of PICs between anionic and cationic polysaccharides has not been reported. The utilization of PIC formation for continuous fiber fabrication by a microfluidic device is technically challenging because PIC formation must be controlled to prevent clogging.

Here, we first demonstrated that both hollow and solid water-insoluble fibers made of PICs of CS and CHI were successfully prepared using the same microfluidic device. The effects of preparation conditions, such as solvent, concentration and flow rate, on the formability, morphology, and dimensions of the fibers were investigated. Furthermore, the loading of proteins in the fibers was examined using bovine serum albumin (BSA) as a model protein.

Materials and methods

Reagents

CS (sodium salt, from shark cartilage, molecular weight (MW) *ca*. 20,000), CHI (from crab shell, MW ≥ 100,000),

fluorescein isothiocyanate (FITC) and other chemicals were purchased from Nacalai Tesque, Inc. BSA, rhodamine B isothiocyanate (RITC) and fluoresceinamine (FA) were obtained from Sigma Co., Ltd. CHI was used after purification (Supplementary Information, method 1), and the other reagents were used without further purification. The distilled water and ultrapure water (18.2 MΩ cm) used in experiments were prepared using Advantec RFD210TA and Advantec RFU414BA, respectively.
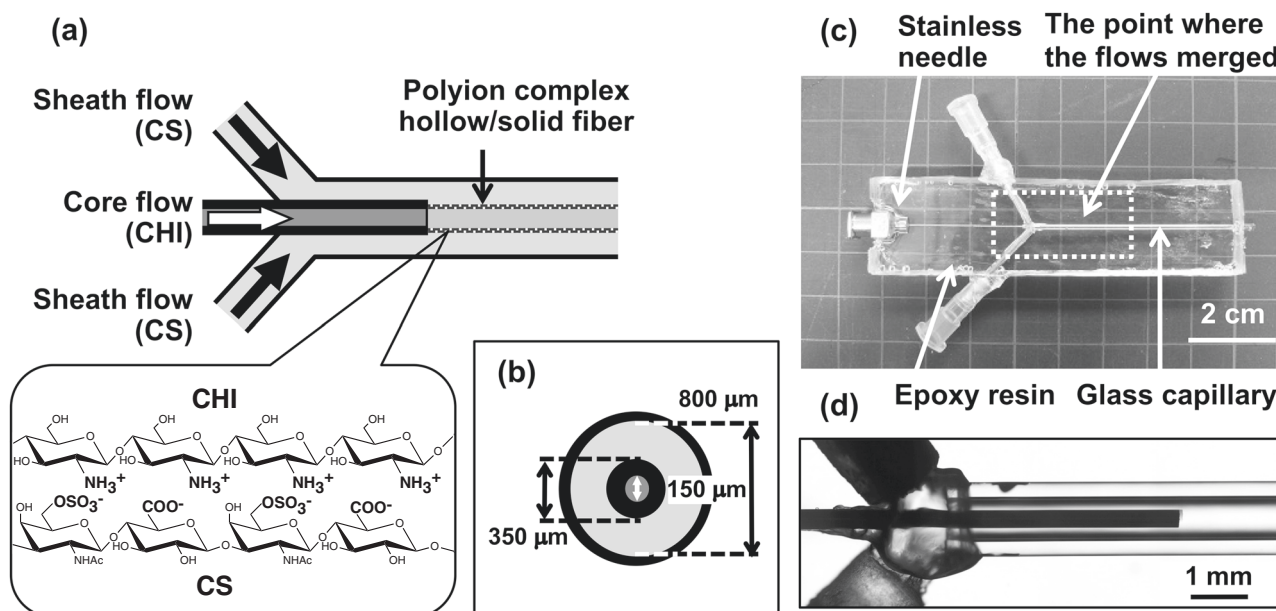
Construction of microfluidic device

Set-up, dimensions, and macroscopic and microscopic views of the microfluidic device are shown in Fig. 1. A stainless-steel 28G needle (inner diameter: 150 μm, outer diameter: 350 μm, length: 28 mm, Kyowa Interface Science, Co. Ltd.) was temporarily fixed inside a capillary tube (inner diameter: 800 μm, outer diameter: 1300 μm, length: 55 mm, Sansyo, Co. Ltd.) using a brass tube (inner diameter: 400 μm, outer diameter: 800 μm), and the root of the capillary tube was coated with silicon grease to make a cavity to connect with the flow paths. These were set in a mold (20 mm × 75 mm × 5 mm) and filled with epoxy resin (Nissin resin, Co. Ltd.). After removing the brass tube, flow paths from both sides of the device to the cavity of the root of glass capillary at the angle of 45° were generated using a drill. A stainless-steel 18G needle (Terumo Corp.) was inserted in the path and fixed with epoxy resin.

Preparation of hollow and solid fibers

To prepare the fibers, 2 or 4 wt% CHI solutions in 2 wt% aqueous acetic acid and 4 wt% CS solutions in ultrapure water or 20% (v/v) ethanol were continuously infused into the core and sheath channels, respectively, at the indicated flow rate using syringe pumps (KDS Legato 110, KD Scientific Inc.). The fabricated fibers were injected into a sheath solution in a glass beaker. For fluorescence microscopic observation, fluorescein-labeled CS (FL-CS, Supplementary Information, method 2 and Figure S1(a)) and rhodamine B-labeled CHI (Rho-CHI, Supplementary Information, method 3 and Figure S1(b)) were blended in the sheath and core solutions at 1/100 (w/w) of both polysaccharides, and the fibers were fabricated in the same manner.

Preparation of protein-incorporated hollow and solid fibers

The indicated amount of BSA was dissolved in 2 wt% aqueous acetic acid with CHI. Hollow and solid fibers were then prepared using the same procedure. For fluorescence

Fig. 1 The microfluidic device used in this study. **a** Schematic illustration of the microfluidic device and the preparation of fibers. **b** Sectioned illustration of the flow exit, and **c**, **d** macroscopic (**c**) and magnified (**d**) views of the microfluidic device

microscopic observation, FITC-labeled BSA (FITC-BSA, Supplementary Information, method 4 and Figure S1(c)) was incorporated in BSA at 1/10 (w/w), and the fibers were fabricated in the same manner.

Characterization

The morphologies of the obtained fibers were observed using a fluorescence microscope (ECLIPSE LV100, Nikon Corp.) combined with a precentered fiber illuminator (Intensilight C-HGFI, Nikon Corp.) and NIS-Elements software (Nikon Corp.). For observation of FL-, FITC-, and Rho-labeled molecules, filters (B-3A (excitation filter (EX): 420–490 nm, dichroic mirror (DM): 505 nm, barrier filter (BA): 520 nm) and FITC filter block (EX: 430–480 nm, DM: 505 nm, BA: 535–545 nm) for FL- and FITC-labeled molecules and G-2A (EX: 510–560 nm, DM: 575 nm, BA: 590 nm) for Rho-labeled molecules) were used. The fibers were observed in the sheath solution unless noted otherwise. Plots of the fluorescence profiles were obtained using ImageJ software [24]. The diameter and thickness of the fibers were calculated from the cross-sectional images of the fibers obtained using NIS-Elements software. The diameter of the fiber was estimated from the geometric mean of the sides of the bounding box of the fibers, and the fiber thickness was estimated from the arithmetic mean of the thickness of three points on the walls. The diameters and thicknesses of at least three independent fibers were measured, and the results are shown as the mean ± standard deviation. For scanning electron microscopy (SEM) observations, fibers prepared using ultrapure water as a solvent of CS were rinsed with ultrapure water and freeze-dried after pre-freezing with liquid nitrogen. Fibers prepared using 20% ethanol as a solvent of CS were dehydrated in acetone for 3 h. Cross-sections of the fibers were observed by SEM (JSM-7001F, JEOL Ltd.) with an acceleration voltage of 20 kV after coating with Pd–Pt using an ion sputter instrument (MC1000, Hitachi Ltd.). Cross-sections that formed during sample handling processes were found in the specimens and observed.

Stability of hollow fibers in solutions

Hollow fibers prepared at a core flow rate of $50\ \mu l\ min^{-1}$ and sheath flow rate of $1000\ \mu l\ min^{-1}$ were immersed in ultra-pure water, phosphate buffer (PB, 10 mM phosphate ion species, pH 5.8, 7.4, 8.0), phosphate buffered saline (PBS, 10 mM phosphate ion species and 137 mM NaCl, pH 7.4), and 2-(N-morpholino) ethanesulfonic acid (MES) buffer (62.5 mM, pH 6.5) for 24 h and were observed in the solutions under optical microscopy.

Evaluation of release behaviors of FITC-BSA from fibers

FITC-BSA-loaded fibers obtained by spinning for 2 min were immersed in 5 ml of ultrapure water and PBS. The samples were then incubated at 36.5 °C using a dry chamber (DOV-750A, AS ONE). The released amounts of

Fig. 2 Microscopic images of CS/CHI composite fibers. Optical images (**a**, **b**) and fluorescent images (**c**, **d** FL-CS, **e**, **f** Rho-CHI) of CS/CHI fibers prepared using water (**a,c,e**) and 20% (v/v) ethanol (**b, d, f**) as a solvent of sheath solution. Flow conditions are as follows. Core: 50 μl min^{-1}, sheath: 1000 μl min^{-1}. Scale bars: 500 μm (**a, b**) and 200 μm (**c–f**)
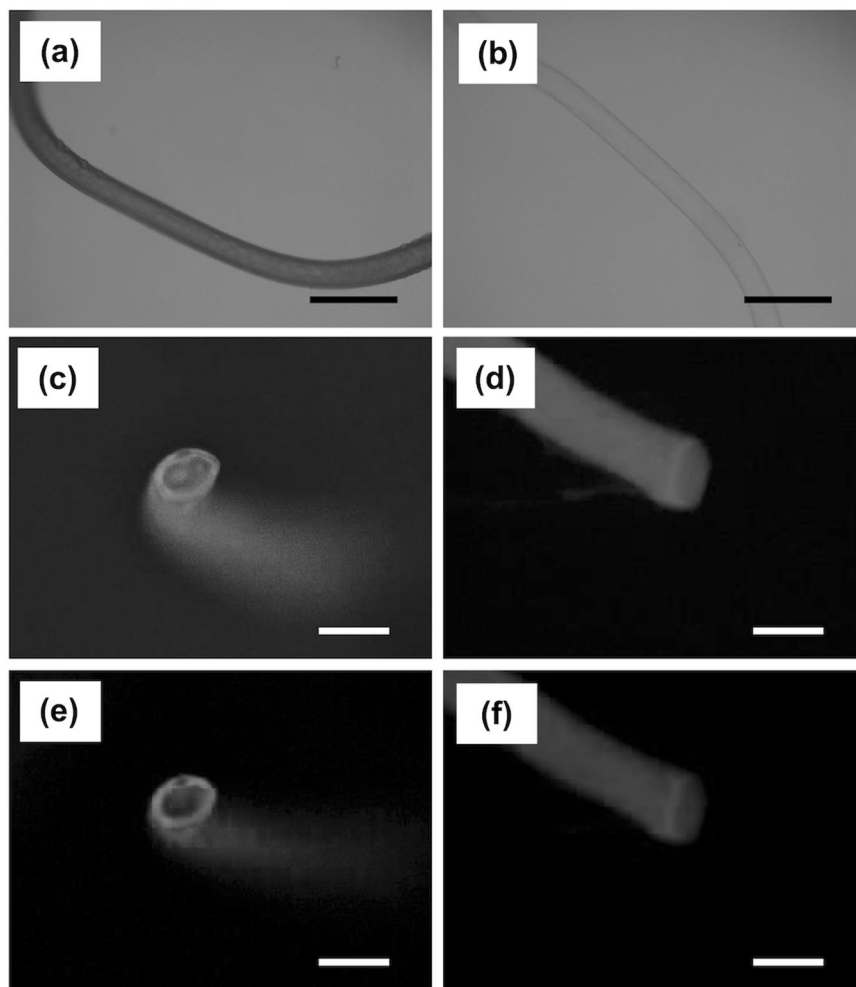
FITC-BSA were evaluated using a UV-vis spectrophotometer (V-660, JASCO Corp.). The absorbance of FITC-BSA at 500 nm was used to calculate the released amounts.

Results

Preparation of CS/CHI composite hollow and solid fibers

A microfluidic device in which the CHI and CS solutions co-axially flow and PICs of CS and CHI can be formed at the interface was designed for the fabrication of hollow and solid polysaccharide composite fibers (Fig. 1a). The microfluidic device with the dimensions shown in Fig. 1b was constructed from a stainless-steel needle and a glass capillary (Fig. 1c, d). First, the conditions under which a stable laminar flow was formed were investigated using 2 wt% CHI solutions in 2 wt% aqueous acetic acid stained with methylene blue (MB) as the core flow and ultrapure water as the sheath flow (Supplementary Information,

method 5 and Figure S2). When the ratio of the face velocities of the core and the sheath flows (core/sheath) was large (*ca.* 5 or more), the core flow was unstable. By contrast, when the ratio was small (*ca.* 0.5 or less), the flow was narrowed. Under the conditions in which the ratio was nearly equal to 1, stable laminar flow was observed. Then, 4 wt% CHI solutions in 2 wt% aqueous acetic acid and 4 wt% CS solutions were continuously infused into the core and the sheath channels at 50 μl min^{-1} (face velocity: 2800 mm min^{-1}) and 1000 μl min^{-1} (face velocity: 2500 mm min^{-1}), respectively. Soft fibers with smooth surfaces were obtained by using ultrapure water (Fig. 2a) and 20% ethanol (Fig. 2b) as the solvent of the sheath solution. To elucidate the distribution of CS and CHI in the fibers, the fibers were prepared by blending FL-CS and Rho-CHI and then observed by fluorescence microscopy. Cross-sectional fluorescence images of the fibers obtained using ultrapure water as a solvent of the sheath solution indicated that the fibers had a hollow structure (Fig. 2c, e). The fibers were composed of both CS and CHI, and these polysaccharides were distributed homogeneously in the wall of the hollow

Fig. 3 SEM images of the cross-section of CS/CHI fibers prepared using water (**a**, **b**) and 20% (v/v) ethanol (**c**, **d**) as a solvent of the sheath solution. **b** and **d** are magnified images of **a** and **c**, respectively. Scale bars: 50 μm (**a**, **c**) and 10 μm (**b**, **d**)
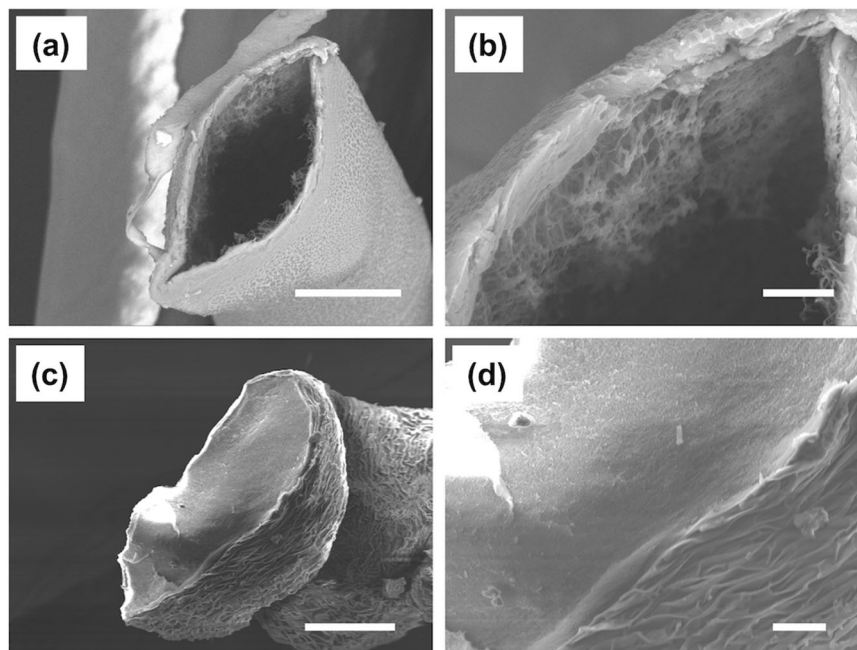
fiber. The mean diameter of the hollow fibers was 168 ± 20 μm and the thickness of the wall was 15.9 ± 4.8 μm. By contrast, the fibers obtained by using 20% ethanol as the solvent of the sheath solution showed a solid structure (Fig. 2d, f). The fibers were also composed of CS and CHI, and these were distributed homogeneously in the fibers. The diameter of the solid fiber was 236 ± 18 μm. SEM observation of freeze-dried or dehydrated fibers showed hollow and solid structures of the obtained fibers (Fig. 3).

The FT-IR spectra of CS/CHI fibers prepared by using ultrapure water (Fig. 4c) and 20% ethanol (Fig. 4d) showed various peaks originating from CS (Fig. 4a) and CHI (Fig. 4b), such as the $C = O$ stretching vibration (*ca.* 1650 cm^{-1}, amide I) [25, 26], N–H stretching vibration (*ca.* 1575 cm^{-1}, amide II) [25, 26], C–H symmetric and asymmetric stretching vibrations (*ca.* 2900 cm^{-1}) [25, 26] and OH stretching vibration (*ca.* 3400 cm^{-1}, broad) [25, 26] in both CS and CHI, and SO_3^- asymmetric stretching vibration (*ca.* 1220 cm^{-1}) [26] in CS. In addition to these peaks, a new peak appeared at 1530 cm^{-1} in the both CS/CHI hollow and solid fibers (denoted by an asterisk (*) in Fig. 4c, d), which supported ion complex formation between the NH_3^+ and COO^- groups [27].

Stability of CS/CHI hollow fibers

Stability of the CS/CHI hollow fibers in various kinds of solvents was investigated. Although morphologies of the fibers did not change after 24-h immersion in PB with pH 5.8 (Fig. 5a), 7.4 (Fig. 5b), and 8.0 (Fig. 5c), PBS (pH 7.4,

Fig. 5d), and MES buffer (pH 6.5, Fig. 5e), the fibers became thicker and partly ruptured after immersion in ultrapure water (Fig. 5f).

The effect of the flow rate on morphology, diameter, and thickness of CS/CHI hollow fibers

The effects of the flow rates of the core and sheath flows on the morphology and dimensions of hollow fibers were investigated with 20% ethanol used as the sheath flow solvent. First, the core flow rate was fixed at 50 μl min^{-1}, while the sheath flow rate was changed. When the sheath flow rate was 500 μl min^{-1}, the surface of the fibers showed a foam-like structure (Fig. 6a). For the flow rates in the 750–2000 μl min^{-1} range, fibers with smooth surfaces were obtained (Fig. 6b–d), and their diameters and thicknesses were decreased by increasing the sheath flow rate (Fig. 7a, c). Then, the sheath flow rate was fixed at 1000 μl min^{-1}, and the core flow rate was changed. Fibers prepared at a core flow rate of 10 μl min^{-1} showed smooth surface, and their diameters and thicknesses were smaller than those obtained at a core flow rate of 50 μl min^{-1} (Fig. 6e). By contrast, fibers with a hairy surface were obtained at a core flow rate of 100 μl min^{-1} (Fig. 6f). The fiber diameter and thickness appeared to be constant for the flow rate greater than 50 μl min^{-1} (Fig. 7b, d). Fibers could be fabricated from 2 wt% CHI solutions in 2 wt% acetic acid. Although there was no significant difference in morphology and its diameter, their walls were thinner than those obtained from 4 wt% of CHI (Fig. 8).
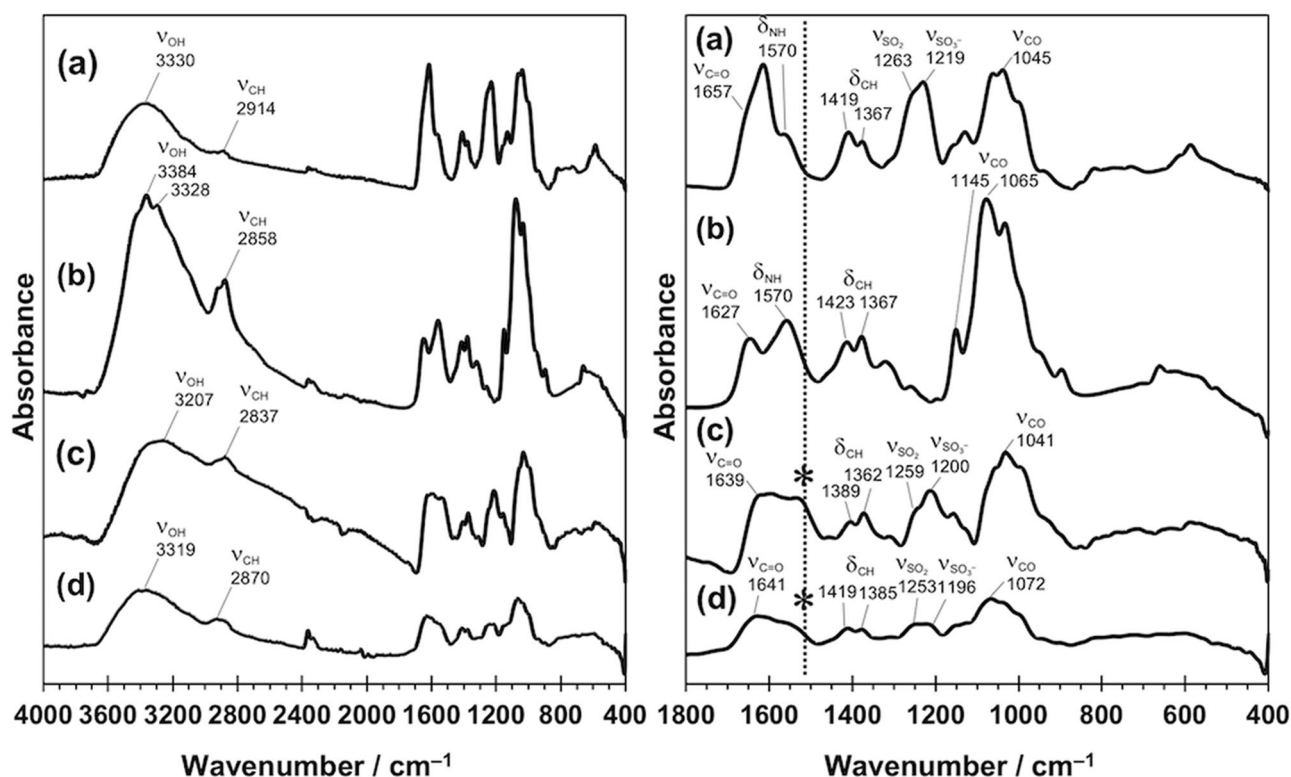
Fig. 4 FT-IR spectra (left) with zoom in the region of 1800–400 cm^{-1} (right) of CS (**a**), CHI (**b**), and CS/CHI fibers prepared using water (**c**) and 20% (v/v) ethanol (**d**) as a solvent of the sheath solution.

Dashed lines show that the position of the peak originated from NH$_3^+$, which is also denoted by an asterisk (*) in (**c**) and (**d**)

Incorporation of proteins in the CS/CHI composite fibers

Polysaccharide composite hollow and solid fibers were also formed when BSA was dissolved in 2 wt% aqueous acetic acid at 0.4 wt% with CHI (Fig. 9a, e). By blending FITC-labeled BSA (FITC-BSA) with BSA, distributions of BSA in the hollow and solid fibers were observed under a fluorescence microscope (Fig. 9b, f). In the hollow fibers, BSA was loaded in internal aqueous phases of the hollow fibers in addition to their walls (Fig. 9b–d′). In the solid fibers, BSA was distributed homogeneously in the fiber (Fig. 9f). The effects of protein loading on the diameter of the fibers were then investigated. Loading of BSA did not affect the diameter of the hollow fibers (Fig. 9g), whereas that of the solid fiber was decreased upon increasing the concentration of BSA (Fig. 9h).

## Release behaviors of FITC-BSA from composite fibers

Figure 10a shows the release behaviors of FITC-BSA from the FITC-BSA-incorporated hollow fibers (Fig. 10b) in ultrapure water and PBS. In ultrapure water, FITC-BSA molecules were released from the fibers within an hour,

whereas the release time reached 4 h in PBS. The equilibrium released amounts were almost the same. After 100 h, the fluorescence from FITC-BSA in the fibers was still observed for both cases (Fig. 10c, d).

Discussion

In the present study, we have continuously fabricated fibers made of PICs of natural polysaccharides, CS and CHI, by utilizing microfluidic techniques. Model experiments using the CHI solution as the core solution and pure water as the sheath solution showed that stable laminar flows were formed when the differences in the face velocity between the core flow and the sheath flow were small (Figure S2). Under optimal flow conditions, it was also confirmed that stable laminar flow was formed at both the point where the two flows merged (Figure S3a) and the terminus of the device (Figure S3b). As expected, hollow fibers were formed by using ultrapure water as a solvent of the sheath solution (Fig. 2c, e). It was assumed that water-insoluble PICs were rapidly formed at the interface between the core and the sheath flows and blocked further mass transport across the PIC layers, resulting in the formation of hollow fibers (the details will be discussed below). By contrast, core-filled,
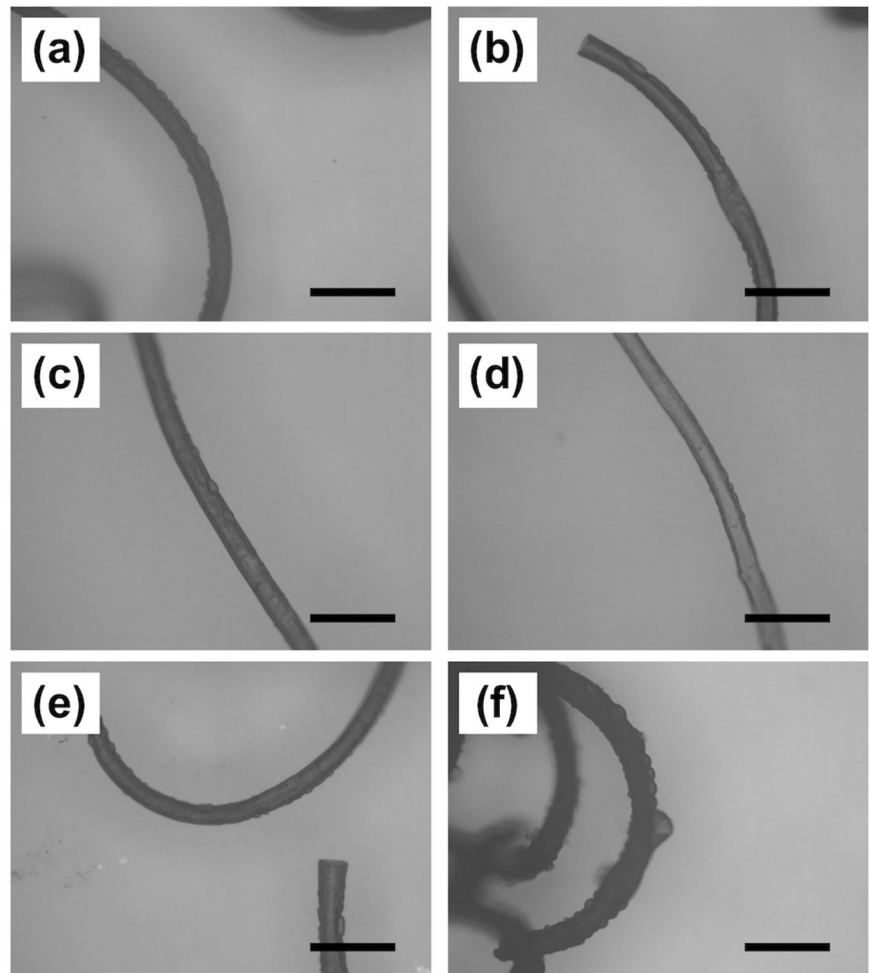
solid fibers were formed by using 20% ethanol as the solvent of the sheath solution (Fig. 2d, f). It has been reported that formation of PIC through electrostatic interaction was weakened in organic solvent such as ethanol [28]. Therefore, CS could diffuse into the more inner region of the core flow in the presence of ethanol, resulting in the formation of homogeneous solid fibers. Preparation of hollow fibers using microfluidics sometimes requires the use of a special device such as the device that generates double-coaxial laminar flows [2, 22]. On the other hand, the present results clearly showed that both hollow and solid fibers made of PICs were successfully prepared on demand using the same microfluidic device. SEM images (Fig. 3) indicated that both hollow and solid fibers swelled in solutions when prepared and could be handled while maintaining their morphologies in the dry state. FT-IR spectra indicated that both hollow and solid fibers had similar chemical composition and were made of PICs of CS and CHI (Fig. 4).

Here, formation of the fibers driven by PIC formation is compared with that driven by electrolyte complex formation of polyelectrolytes and metal ions. In previous reports on ALG-Ca^{2+} fibers, both hollow and solid fibers could be fabricated [20–22]. Coaxial flow using a core flow of ALG and a sheath flow of Ca^{2+} produced solid fibers [20] whereas adverse flow condition (core: Ca^{2+}, sheath: ALG) produced hollow fibers [21]. The use of three-layered coaxial fluids (central: Ca^{2+}, inner: ALG, outer: Ca^{2+}) also made the fibers hollow [22]. This may also be due to high diffusivity of Ca^{2+}. Ca^{2+} can diffuse fast and ALG are solidified, and therefore the obtained fiber reflected the shape of ALG flow. For fiber formation by PICs, once PIC walls were formed at the interface, polysaccharides with high MW could not diffuse across the PIC walls, resulting in formation of hollow fibers.

The obtained CS/CHI composite hollow fibers showed high stability in a variety of biological solutions except ultrapure water (Fig. 5). This is important for the use of these fibers as biomaterials. Instability of the fibers in ultrapure water may be attributed to rupture after the uptake of abundant water.

An increase of the flow rate of the sheath CS solution or a decrease of the flow rate of the core CHI solution reduced the diameters and thicknesses of hollow fibers (Figs 6, 7). The decrease in the diameter with increasing sheath flow

Fig. 6 Microscopic images of CS/CHI composite hollow fibers prepared under various flow conditions. **a** Core: 50 µl min^{-1} (face velocity: 2800 mm min^{-1}), sheath: 500 µl min^{-1} (face velocity: 1200 mm min^{-1}); **b** Core: 50 µl min^{-1}, sheath: 750 µl min^{-1} (face velocity: 1800 mm min^{-1}); **c** Core: 50 µl min^{-1}, sheath: 1000 µl min^{-1} (face velocity: 2500 mm min^{-1}); **d** Core: 50 µl min^{-1}, sheath: 2000 µl min^{-1} (face velocity: 4900 mm min^{-1}); **e** Core: 10 µl min^{-1} (face velocity: 570 mm min^{-1}), sheath: 1000 µl min^{-1}; **f** Core: 100 µl min^{-1} (face velocity: 5700 mm min^{-1}), sheath: 1000 µl min^{-1}. Scale bars: 500 µm
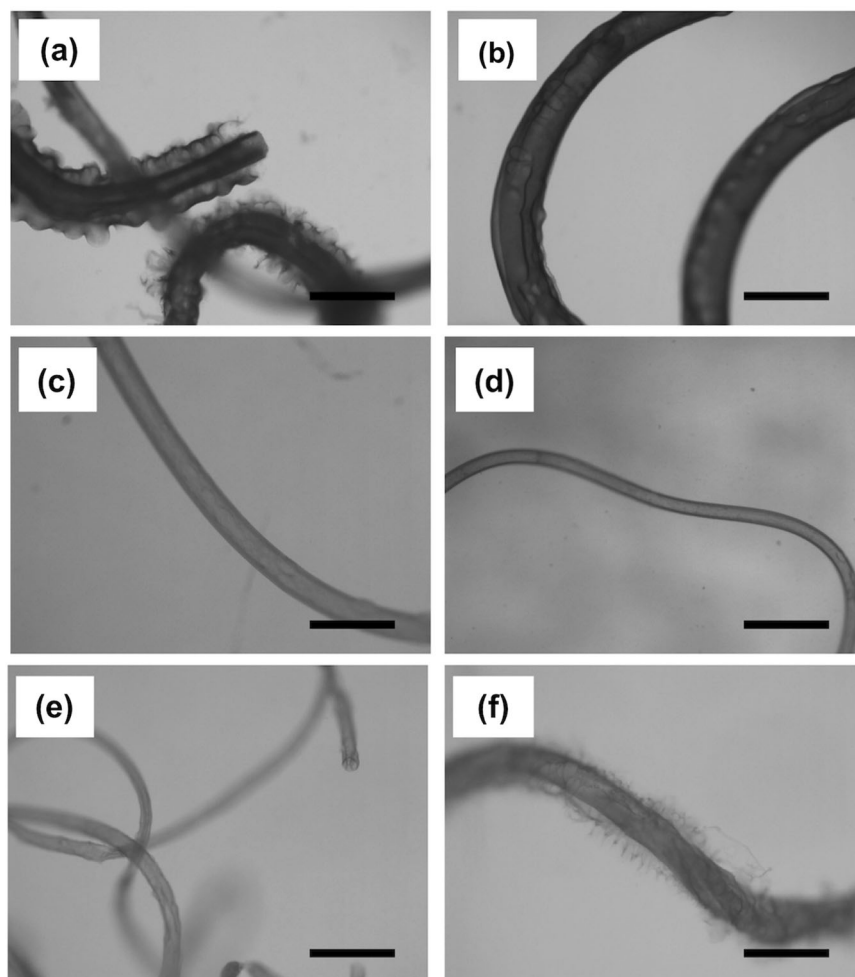

rate and decreasing core flow rate have been reported for other fibers prepared with microfluidics [18, 21, 29, 30], and it can be explained that the increasing difference in the face velocities of the core and the sheath flows induced a larger drag force and stretched the core solution. If the difference in the face velocities was too large, the laminar flow was destabilized and transformed to turbulent flow (Figure S2). Instability of the flow resulted in the formation of fibers with foam-like or hairy surfaces (Figs. 6a, f). Furthermore, the thickness of the hollow fibers depended on the concentration of the CHI solutions (Fig. 8b). These results suggested that the diameter and thickness of hollow fibers can be controlled by changing the flow conditions within the limits of a certain range.

Polysaccharide composite hollow and solid fibers containing proteins were also prepared by adding the proteins into the core flow of the CHI solutions. The proteins were loaded in PICs by electrostatic interaction and hydrogen bonding, and the system was widely used for protein delivery and their controlled release [31]. We have demonstrated that BSA were loaded in PIC complex gels of CS and CHI by mixing BSA in CHI solutions (unpublished data). Since BSA with isoelectric point of 4.7 [32] were positively charged in 2 wt% acetic acid solutions, complexes of BSA and CHI were not formed in the CHI solutions. During fiber formation, BSA interacted with CS or became negatively charged in the neutral solution and interacted with CHI. Alternatively, BSA was simply trapped in the PIC networks prior to diffusing out of the networks because of their relatively rapid formation. Morphological observations showed that incorporation of BSA into the fibers did not change their surface. In the hollow fibers, FITC-BSA was incorporated not only in the walls but also in the internal aqueous phases (Fig. 9b–d). This may be because unloaded BSA molecules were trapped in the internal aqueous phases of the hollow fibers. These results also supported the fast formation of PICs at the interface between the core and sheath flows. By contrast, FITC-BSA molecules were distributed homogeneously in the solid fibers (Fig. 9f). The mean diameter of the solid fibers was decreased by increasing the loaded concentration of BSA (Fig. 9h), whereas that of the hollow fibers was not changed

Fig. 7 Effects of the sheath flow rate (**a**, **c**) and core flow rate (**b**, **d**) on the diameter (**a**, **b**) and thickness (**c**, **d**) of the composite hollow fibers. The core flow rate in **a** and **c** was 50 µl min^{-1}, and the sheath flow rate in (**b**) and (**d**) was 1000 µl min^{-1}, respectively. Error bars indicate the standard deviation (SD) ($n > 3$). *Significant ($p < 0.05$, Student's t-test)
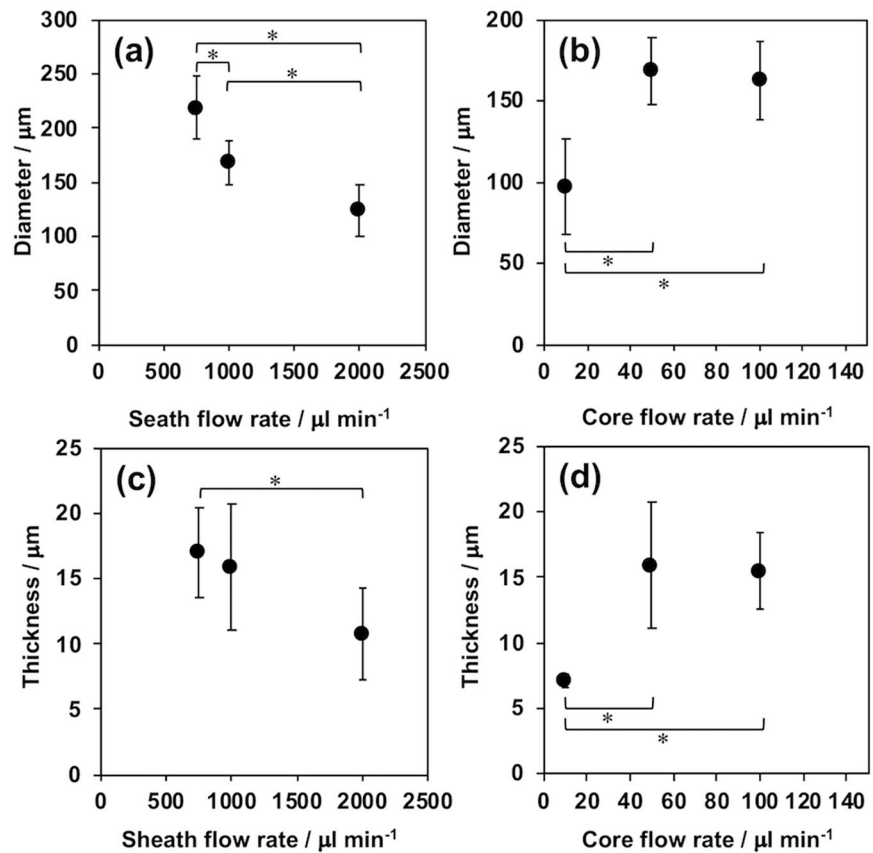
Fig. 8 Effects of concentration of CHI used as the core flow on the diameter (**a**) and thickness (**b**) of the composite hollow fibers. The core flow rate was fixed at 50 µl min^{-1}, and the sheath flow rates were 1000 and 2000 µl min^{-1}. Error bars indicate the standard deviation (SD) ($n > 3$). NS not significant, using the Student's t-test
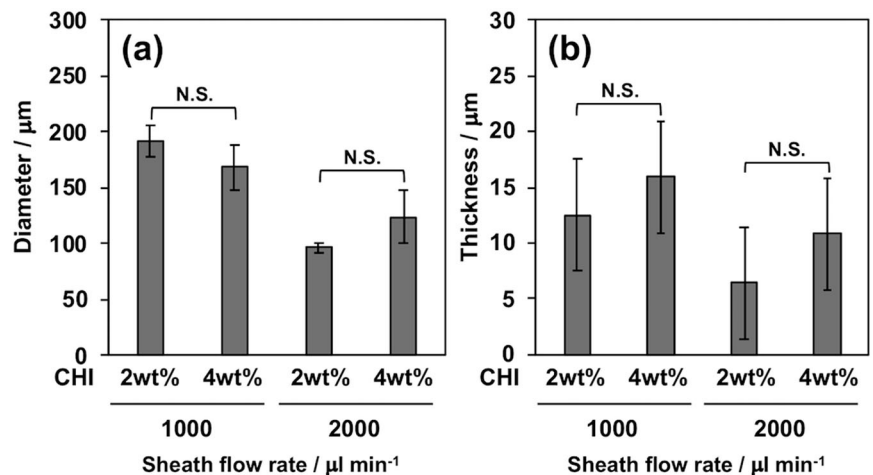
(Fig. 9g). Incorporation of BSA can affect the electrostatic interaction between CS and CHI, which may induce a decrease in fiber diameter.

Regarding the release behaviors of FITC-BSA loaded in hollow fibers, release in ultrapure water was faster than that in PBS whereas their equilibrium release amounts were almost the same. Fast release in ultrapure water appeared to be due to a burst release of FITC-BSA from the internal aqueous phase of the hollow fibers and correlated with the

difference in the stability of the fibers in ultrapure water and PBS. The fact that FITC-BSA remained in the fibers after 100 h immersion in PBS and ultrapure water (Fig. 10c, d) indicated that the FITC-BSA molecules located inside the wall of fibers may strongly interact with the PICs. Continuous, long-time release of proteins may be achieved if we can gradually weaken the interactions.

Although compounds with low MW, such as MB, could also be loaded in the CS/CHI hollow fibers, these were
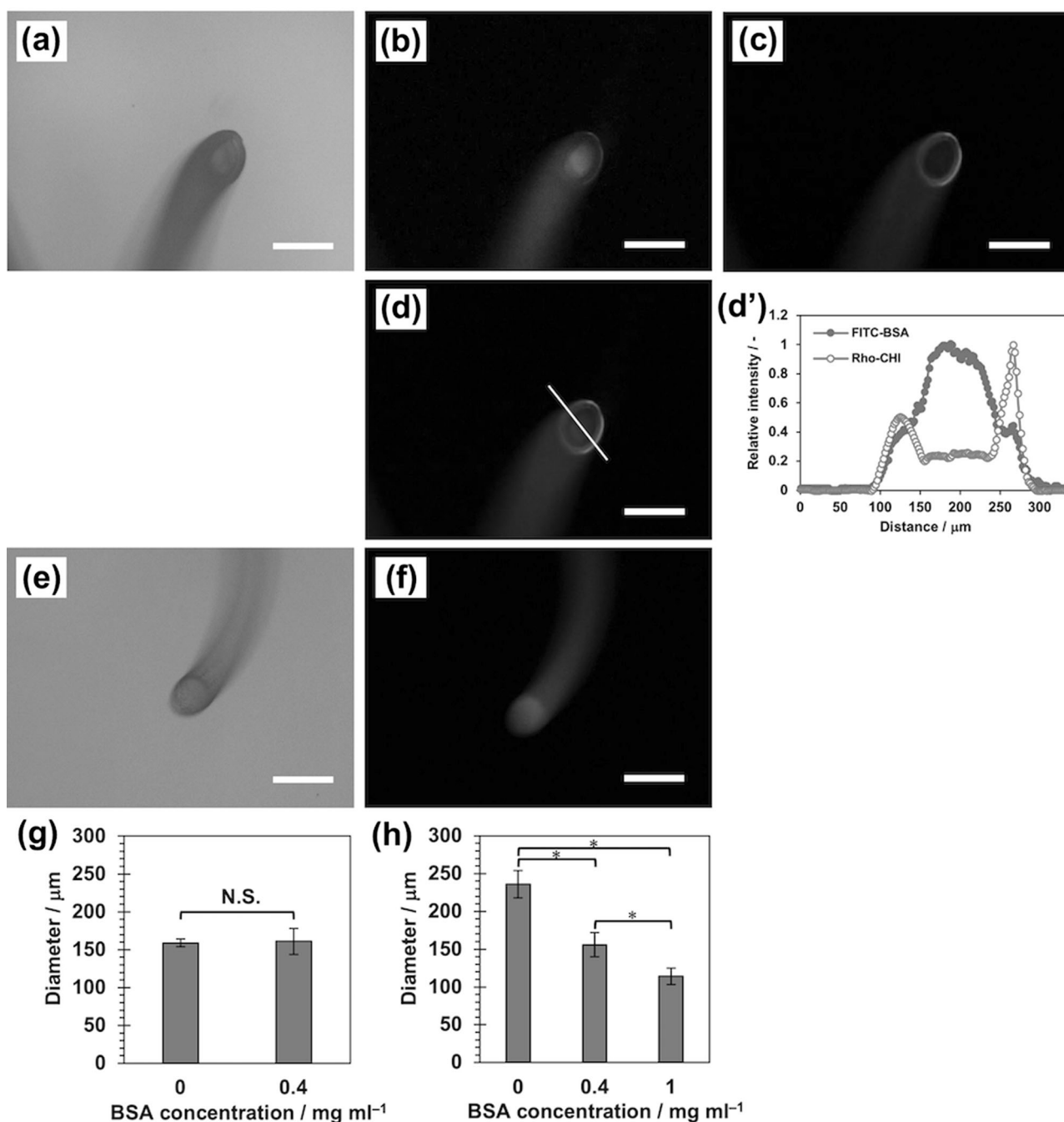
Fig. 9 FITC-BSA-loaded CS/CHI composite fibers. **a–f** Microscopic images of CS/CHI composite fibers prepared using water (**a–d**) and 20% (v/v) ethanol (**e, f**) as a solvent of the sheath solution. **a–d** Optical images (**a**), and fluorescent images of FITC-BSA (**b**), Rho-CHI (**c**), and the overlay image (**d**). Plots of fluorescence profiles in (**d**) are shown in (**d'**). **e, f** Optical images (**e**), and fluorescent images of FITC-

BSA (**f**). **g, h** Effect of BSA concentration on diameter of the composite fibers prepared using water (**g**) and 20% (v/v) (**h**) as the solvent of the sheath solution. Scale bars: 200 μm. Error bars indicate the standard deviation (SD) ($n > 3$). *Significant ($p < 0.05$, Student's t-test). NS not significant, using the Student's t-test

released to the coagulation solution immediately after spinning (Supplementary Information, method 6 and Figure S4). These results suggested that release from the fibers were correlated with the interaction between the model drugs and polysaccharides and the diffusivity of model drugs in the polysaccharides PICs. In fact, we previously demonstrated

that MB loaded in CS/CHI composite films prepared by hot-pressing PIC gels were readily released from the films within 1 h [33], in contrast to FITC-BSA released continuously for up to 2 weeks. One possible solution for the loading of small MW compounds in the present fibers is the use of nanosized reservoirs. For example, coumarin 6 was successfully

Fig. 10 Release behaviors of FITC-BSA from the FITC-BSA-incorporated hollow fibers in PBS and ultrapure water. **a** Released amount of FITC-BSA from hollow fibers. **b–d** Fluorescence microscopy images of FITC-BSA-incorporated hollow fibers before (**b**) and after immersion in PBS (**c**) and water (**d**) for 100 h. Scale bars: 500 μm
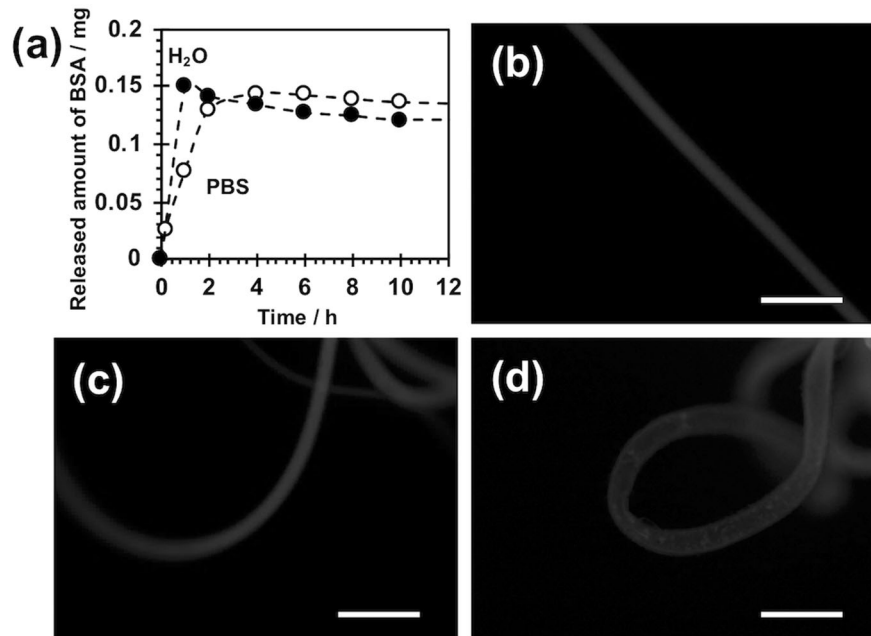
incorporated in the hollow fibers by loading coumarin 6 in polylactic acid nanoparticles that added in the core flows (Figure S5). Since polylactic acid is biodegradable, such a system can be expected to realize a sustained release of small MW drugs. The ability of CS/CHI fibers to stably hold proteins and nanomaterials allows the functionalization of the fibers with bioactive molecules such as growth factors, cell adhesion proteins and drugs. These molecules should be released according to their desired profiles based on the knowledge of the design and fabrication of various drug delivery systems.

Conclusion

Although polysaccharides and their PICs are promising materials for biomedical applications, their fabrication processes are limited. In this study, we demonstrated that distinct hollow and solid fibers made of PICs of CS and CHI could be fabricated using the same microfluidic device by merely changing the sheath flow solvent. The diameters of the fibers were also controllable depending on the flow rate. Furthermore, proteins could be incorporated in the hollow and solid fibers by mixing them in the core flow solutions. CS-based materials have been used for regeneration of wide range of tissues, cartilage [34], bone [35], skin [36], and nerve [37]; therefore, CS/CHI composite fibers are potent materials for use in tissue engineering. We are currently conducting cell culture experiments using the present fibers. PICs of polysaccharides have been prepared from not only CS but also other glycosaminoglycans

(GAGs) such as hyaluronic acid and heparin with CHI [38]. This means that hollow and solid fibers with various biological functions could also be fabricated from other GAGs using microfluidic techniques.

Compliance with ethical standards

Conflict of interest The authors declare that they have no conflict of interest.

References

1. Iwasaki N, Kasahara Y, Yamane S, Igarashi T, Minami A, Nisimura S. Chitosan-based hyaluronic acid hybrid polymer fibers as a scaffold biomaterial for cartilage tissue engineering. Polymers. 2011;3:100–13.
2. Onoe H, Okitsu T, Itou A, Kato-Negishi M, Gojo R, Kiriya D, Sato K, Miura S, Iwanaga S, Kuribayashi-Shigetomi K, Matsunaga YT, Shimoyama Y, Takeuchi S. Metre-long cell-laden microfibres exhibit tissue morphologies and functions. Nat Mater. 2013;12:584–90.
3. Daly W, Yao L, Zeugolis D, Windebank A, Pandit A. A biomaterials approach to peripheral nerve regeneration: bridging the peripheral nerve gap and enhancing functional recovery. J R Soc Interface. 2012;9:202–21.
4. Kakisis JD, Liapis CD, Breuer C, Sumpio BE. Artificial blood vessel: the Holy Grail of peripheral vascular surgery. J Vasc Surg. 2005;41:349–54.
5. Tharakan JP, Chau PC. A radial flow hollow fiber bioreactor for the large-scale culture of mammalian cells. Biotechnol Bioeng. 1986;28:329–42.

6. Shelke NB, James R, Laurencin CT, Kumbar SG. Polysaccharide biomaterials for drug delivery and regenerative engineering. Polym Adv Technol. 2014;25:448–60.

7. Tokura S, Nishi N, Noguchi J. Studies on chitin. III. Preparation of chitin fibers. Polym J. 1979;11:781–6.

8. Knaul J, Hooper M, Chanyi C, Creber AMK. Improvements in the drying process for wet-spun chitosan fibers. J Appl Polym Sci. 1998;69:1435–44.

9. Li L, Yuan B, Liu S, Yu S, Xie C, Liu F, Guo X, Pei L, Zhang B. Preparation of high strength chitosan fibers by using ionic liquid as spinning solution. J Mater Chem. 2012;22:8585–93.

10. Barber PS, Griggs CS, Bonner JR, Rogers RD. Electrospinning of chitin nanofibers directly from an ionic liquid extract of shrimp shells. Green Chem. 2013;15:601–7.

11. Ohkawa K, Cha D, Kim H, Nishida A, Yamamoto H. Electro-spinning of chitosan. Macromol Rapid Commun. 2004;25:1600–5.

12. Amaike M, Senoo Y, Yamamoto H. Sphere, honeycomb, regularly spaced droplet and fiber structures of polyion complexes of chitosan and gellan. Macromol Rapid Commun. 1998;19:287–9.

13. Yamamoto H, Ohkawa K, Nakamura E, Miyamoto K, Komai T. Preparation of polyion complex capsule and fiber of chitosan and gellan-sulfate at aqueous interface. Bull Chem Soc Jpn. 2003;76:2053–7.

14. Iijima K, Yuyama K, Asaine K, Irie K, Hashizume M. Preparation of chondroitin sulfate/chitosan composite fibers by spinning from aqueous solution interfaces. Kobunshi Ronbunshu. 2014;71:11–16.

15. Wang JZ, Huang XB, Xiao J, Li N, Yu WT, Wang W, Xie WY, Ma XJ, Teng YL. Spray-spinning: a novel method for making alginate/chitosan fibrous scaffold. J Mater Sci Mater Med. 2010;21:497–506.

16. Sackmann EK, Fulton AL, Beebe DJ. The present and future role of microfluidics in biomedical research. Nature. 2014;507:181–9.

17. Jun Y, Kang E, Chae S, Lee SH. Microfluidic spinning of micro- and nano-scale fibers for tissue engineering. Lab Chip. 2014;14:2145–60.

18. Sakai S, Liu Y, Mah EJ, Taya M. Horseradish peroxidase/cata-lase-mediated cell-laden alginate-based hydrogel tube production in two-phase coaxial flow of aqueous solutions for filament-like tissues fabrication. Biofabrication. 2013;5:015012.

19. Choi CH, Yi H, Hwang S, Weitz DA, Lee CS. Microfluidic fabrication of complex-shaped microfibers by liquid template-aided multiphase microflow. Lab Chip. 2011;11:1477–83.

20. Shin SJ, Park JY, Lee JY, Park H, Park YD, Lee KB, Whang CM, Lee SH. "On the Fly" continuous generation of alginate fibers using a microfluidic device. Langmuir. 2007;23:9104–8.

21. Pham HTU, Hanif M, Asthana A, Iqbal MS. A microfluidic device approach to generate hollow alginate microfibers with controlled wall thickness and inner diameter. J Appl Phys. 2015;117:214703.

22. Lee KH, Shin SJ, Park Y, Lee SH. Synthesis of cell-laden alginate hollow fibers using microfluidic chips and microvascularized tissue-engineering applications. Small. 2009;5:1264–8.

23. Lee KH, Shin SJ, Kim CB, Kim JK, Cho YW, Chung BG, Lee SH. Microfluidic synthesis of pure chitosan microfibers for bio-artificial liver chip. Lab Chip. 2010;10:1328–34.

24. Schneider CA, Rasband WS, Eliceiri KW. NIH Image to ImageJ: 25 years of image analysis. Nat Methods. 2012;9:671–5.

25. Kasaai MR. A review of several reported procedures to determine the degree of N-acetylation for chitin and chitosan using infrared spectroscopy. Carbohydr Polym. 2008;71:497–508.

26. Huang Z, Nooeaid P, Kohl B, Roether JA, Schubert DW, Meier C, Boccaccini AR, Godkin O, Ertel W, Arens S, Schulze-Tanzil G. Chondrogenesis of human bone marrow mesenchymal stromal cells in highly porous alginate-foams supplemented with chondroitin sulfate. Mater Sci Eng C Mater Biol Appl. 2015;50:160–72.

27. Kikuchi Y, Noda A. Polyelectrolyte complexes of heparin with chitosan. J Appl Polym Sci. 1976;20:2561–3.

28. Abe K, Ohno H, Nii A, Tsuchida E. Calorimetric study on the formation of polymer complexes through electrostatic interaction and hydrogen bonding. Macromol Chem Phys. 1978;179:2043–50.

29. Sakai S, Kawabata K, Ono T, Ijima H, Kawakami K. Higher viscous solution induces smaller droplets for cell-enclosing cap-sules in a co-flowing stream. Biotechnol Prog. 2005;21:994–7.

30. Takei T, Sakai S, Ijima H, Kawakami K. Development of mam-malian cell-enclosing calcium-alginate hydrogel fibers in a co-flowing stream. Biotechnol J. 2006;1:1014–7.

31. Cooper CL, Dubin PL, Kayitmazer AB, Turksen S. Polyelectrolyte–protein complexes. Curr Opin Colloid Interface Sci. 2005;10:52–78.

32. Malamud D, Drysdal JW. Isoelectric points of proteins: a table. Anal Biochem. 1978;86:620–47.

33. Hashizume M, Murata Y, Shibata T, Iijima K. Drug loading and release behaviors of freestanding polysaccharide composite films. Polym J. 2016;48:545–50.

34. Ko CS, Huang JP, Huang CW, Chu IM. Type II collagen-chondroitin sulfate-hyaluronan scaffold cross-linked by genipin for cartilage tissue engineering. J Biosci Bioeng. 2009;107:177–82.

35. Yang S, Guo Q, Shores LS, Aly A, Ramakrishnan M, Kim GH, Lu Q, Su L, Elisseeff JH. Use of a chondroitin sulfate bioadhesive to enhance integration of bioglass particles for repairing critical-size bone defects. J Biomed Mater Res A. 2015;103:235–42.

36. Yan S, Zhang Q, Wang J, Liu Y, Lu S, Li M, Kaplan DL. Silk fibroin/chondroitin sulfate/hyaluronic acid ternary scaffolds for dermal tissue reconstruction. Acta Biomater. 2013;9:6771–82.

37. Xu H, Yan Y, Li S. PDLLA/chondroitin sulfate/chitosan/NGF conduits for peripheral nerve regeneration. Biomaterials. 2011;32:4506–16.

38. Hashizume M, Kobayashi H, Ohashi M. Preparation of free-standing films of natural polysaccharides using hot press techni-que and their surface functionalization with biomimetic apatite. Colloids Surf B. 2011;88:534–8.